Since January 2020 Elsevier has created a COVID-19 resource centre with free information in English and Mandarin on the novel coronavirus COVID-19. The COVID-19 resource centre is hosted on Elsevier Connect, the company's public news and information website.

Cities 129 (2022) 103808

Contents lists available at ScienceDirect

Cities

journal homepage: www.elsevier.com/locate/cities

Sensing global changes in local patterns of energy consumption in cities during the early stages of the COVID-19 pandemic

Francisco Rowe [a,*], Caitlin Robinson [b], Nikos Patias [a]

[a] Geographic Data Science Lab, Department of Geography and Planning, University of Liverpool, Liverpool, United Kingdom
[b] School of Geographical Sciences, University of Bristol, Bristol, United Kingdom

ARTICLE INFO

Keywords:
COVID-19
Urban energy use
Mobility
Night-time light satellite imagery
Cities

ABSTRACT

COVID-19, and the wider social and economic impacts that a global pandemic entails, led to unprecedented reductions in energy consumption globally. Whilst estimates of changes in energy consumption have emerged at the national scale, detailed sub-regional estimates to allow for global comparisons are less developed. Using night-time light satellite imagery from December 2019–June 2020 across 50 of the world's largest urban conurbations, we provide high resolution estimates (450 m^2) of spatio-temporal changes in urban energy consumption in response to COVID-19. Contextualising this imagery with modelling based on indicators of mobility, stringency of government response, and COVID-19 rates, we provide novel insights into the potential drivers of changes in urban energy consumption during a global pandemic. Our results highlight the diversity of changes in energy consumption between and within cities in response to COVID-19, moderating dominant narratives of a shift in energy demand away from dense urban areas. Further modelling highlights how the stringency of the government's response to COVID-19 is likely a defining factor in shaping resultant reductions in urban energy consumption.

1. Introduction

COVID-19, and the wider social and economic impacts associated with a global pandemic, substantially reconfigured energy consumption patterns (Ruan et al., 2020), causing the biggest fall in global energy investment in history (International Energy Agency (IEA), 2020). With GDP shrinking by −3.3 % globally during 2020 and recoveries diverging (International Monetary Fund (IMF), 2021), energy demand fell by −4 % -in 2020 compared to 2019 levels, impacting advanced economics most severely (IEA, 2021). Global CO2 emissions also fell by −5.8 % during 2020 relative to 2019 (IEA, 2020). Subsequently, Kanda and Kivimaa (2020) characterise COVID-19 as a 'landscape shock' during which rapid political action and emergency legislation - what energy transitions literature terms 'disruptive policies' (Geels et al., 2017) - have shaped the trajectory of energy transitions in unprecedented ways. Where previously government efforts to operationalise low carbon policies have been critiqued as slow and ineffectual, responses to COVID-19 have been characterised by suddenness and scale. Arguably cities have been central to these shifts (Batty, 2020; Connolly et al., 2020). However, there is evidence that many changes are temporary as CO2 emissions returned to pre-pandemic levels during 2021 (Zheng et al., 2020).

The impact of COVID-19 on the wider energy system is an inherently geographical process, rearranging existing distributions, and scales, of socio-economic activity (Kuzemko et al., 2020). As such, like many aspects of the pandemic, energy consumption changes are socially, spatially and temporally uneven. During the early stages of the pandemic new energy consumption practices emerged as societies locked down to differing extents, energy-intensive industries were suspended and people spent a greater proportion of time at home. These patterns were especially stark in cities where energy and associated infrastructures are an integral part of life. In many contexts evidence emerged of a subsequent shift in consumption from commercial, industrial and transportation energy sectors into the domestic sphere (Chen et al., 2020). Coupled with accelerated drops in energy prices (Norouzi et al., 2020), these reconfigurations have tested the finances and flexibility of electricity grids (Kanda & Kivimaa, 2020). Existing energy-related inequalities between and within countries have also been exacerbated as the negative impacts of the pandemic on finances and health disproportionately impacted those who are already least sufficient in terms of domestic energy and mobility (Brosemer et al., 2020; Broto & Kirshner, 2020; Gebreslassie, 2020; Memmott et al., 2021).

To better understand the impact of COVID-19 on energy

* Corresponding author.
E-mail address: f.rowe-gonzalez@liverpool.ac.uk (F. Rowe).

https://doi.org/10.1016/j.cities.2022.103808
Received 8 October 2021; Received in revised form 9 March 2022; Accepted 2 June 2022
Available online 16 June 2022

consumption, national-scale evidence has emerged (Bahmanyar et al., 2020; Gillingham et al., 2020; Ruan et al., 2020). However, changes in energy consumption are likely to be highly locally specific, varying according to socio-economic and urban structure, geographic context, and institutional or cultural change stimulated by COVID-19 (Kanda & Kivimaa, 2020). Subsequently, Acuto et al. (2020) make the case for "seeing COVID-19 like a city" recognising the need to reach "beyond the confines of state-centric views to embrace the political-economic complexity of the 'urban'" (p. 978). In the absence of detailed administrative energy-related statistics, night-time light (NTL) satellite imagery can provide timely evidence of sub-regional changes in energy consumption during the pandemic (Beyer et al., 2021; Bustamante-Calabria et al., 2021; Green et al., 2021). NTL satellite imagery captures the intensity of visible lighting as observed from space. It can detect NTL emissions produced by artificial lighting in cities (e.g. buildings and transport hubs), moonlight and light reflected on the Earth's surface (e.g. snow, water and vegetation) (Levin et al., 2020). Whilst artificial city lighting encoded in NTL satellite imagery does not provide direct estimates of energy consumption, it can effectively capture changes in the spatial distribution of energy intensity over time. Hence, NTL satellite imagery data have been widely used for assessing electrification, detecting and monitoring power outages resulting from natural hazards, such as solar activity, earthquakes, winter storms, strong winds and tornadoes (Arribas-Bel et al., 2022; Min et al., 2013; Román et al., 2019; Wang et al., 2018), and can be an effective tool to capture changes in energy use during the COVID-19 pandemic (Green et al., 2021).

With this in mind, our analysis uses an urban lens to understand how patterns of energy consumption change in response to the pandemic via analysis of detailed NTL satellite imagery, focusing on 50 of the largest global cities. During the early stages of the pandemic, COVID-19 spread rapidly across the world via (inter)national linkages between major global cities, yet as the pandemic has progressed COVID-19 has reached deeper into rural and peri-urban areas with "planetary implications" (Acuto et al., 2020). Our analysis focuses on the early stages of the pandemic, allowing us to evaluate how energy consumption in cities around the world changed in response to the pandemic as it first unfolded. We analyse NTL imagery from three months before and after 11th March 2020 (i.e. December 2019–June 2020), the date on which the World Health Organisation (WHO) declared COVID-19 a global pandemic. Although a global pandemic was not declared until March, city-scale lockdowns in some Chinese cities came into force in late January. Furthermore, in many countries around the world there was a significant lag between the timing of the first registered COVID cases and implementation of non-pharmaceutical interventions. By including imagery from January 2020 and February 2020 in our analysis (and comparing it with a December 2019 baseline) we are able to capture a greater level of spatio-temporal variation in change. Our results therefore provide high-resolution estimates of spatiotemporal changes in urban energy consumption in response to COVID-19. To offer novel insights into potential drivers of changes in NTL intensity, we contextualise imagery with a range of sub-regional indicators of population density, COVID-19 cases and deaths, mobility estimates, and government response indicators. In doing so, the paper:

1. analyses city-scale changes in energy consumption in response to COVID-19;
2. identifies shifts in the spatial patterns of intra-urban energy consumption;
3. explores potential explanations for changes in urban energy consumption.

2. Materials and methods

We analyse the patterns of energy consumption change in 50 of the largest global cities. A list of the cities is provided in the Supplementary Material (SM) Table 1. Three reasons underpin our selection of cities. First, with the exception of Milan (Italy) (included as an epicentre of the initial COVID-19 outbreak), all cities rank within the top 110 largest urban agglomerations based on population size, with over 4.2 million estimated inhabitants in 2020 (United Nations, 2018), to ensure some level of consistency comparing cities of equivalent size. Second, we sought to provide a diverse geographically perspective. Selected cities represent a diversity of national contexts across the Global North and Global South. In countries with a number of large cities we typically select a single representative city to ensure as diverse a national sample as possible. Third, we also seek to identify similarities and differences in the effects of COVID-19 on urban energy use globally. City extents are defined using Functional Urban Area (FUA) boundaries which provide a consistent classification based on density and commuting flows (Schiavina et al., 2019). Our analytical framework consists of four main stages. Each of these stages is in turn described below.

We adopted an open and reproducible research approach based on the use of open software for satellite imagery and statistical analysis - see Code Availability section. As indicated below, all data were obtained from publicly available sources and organised in the form of an open data package - see Data Availability section. We followed best practices in geographic data science (Brunsdon & Comber, 2021) and produce an open data product (Arribas-Bel et al., 2021), including software code to reproduce or extend our analysis, which is available for download as indicated in the Code Availability section.

2.1. Night-time light (NTL) imagery analysis

To understand changes in energy consumption in response to the pandemic in each city, we analyse NTL satellite imagery. NTL imagery captures daily and detailed nocturnal visible light observations of the Earth, providing a unique source to monitor the spatial distribution and intensity variations of human activity at local and planetary scales in near-real time. In addition to street lighting, NTL satellite imagery captures any type of visible light emanating from residential buildings, vehicles, car parks, offices, factories and illuminated sporting venues. NTL data have extensively been used to study electricity consumption, socio-economic activities, light pollution, urban extent changes and power outages (Levin et al., 2020). In the context of COVID-19, NTL imagery has been used to understand the initial impact on the US electricity sector (Ruan et al., 2020), changes in CO2 emissions nationally (Zheng et al., 2020), changes in economic activity in the core of global megacities (Xu et al., 2021), and changes in energy use during the COVID-19 pandemic in specific Brazilian (Carvalho et al., 2021) and European cities (Werth et al., 2021).

We use a monthly composite of NTL data produced by the Payne Institute for Public Policy under the Colorado School of Mines (https://payneinstitute.mines.edu/eog/nighttime-lights/). We utilise the version 1 monthly series of global average radiance composite images from the Visible Infrared Imaging Radiometer Suite (VIIRS) Day-Night Band (DNB) sensor on the Suomi National Polar-orbiting Partnership satellite. The DNB encodes records of visible near-infrared NTL intensity which is measured in radiance units i.e. nanoWatts/cm^2/sr ($nWcm^{-2}sr^{-1}$). The spatial resolution of VIIRS data is 15 arc sec (450 m) across the latitudinal zone of 65°S-75°N5, providing global coverage with 12 hr revisit time (Cao et al., 2017) and a local overpass time of 01:30 am (Elvidge et al., 2013). The data version in our study is the monthly VIIRS Cloud Mask product. These data are corrected for stray light as well as the effects of biogeophysical processes, such as seasonal vegetation and snow (Miller et al., 2013). However, the data are not corrected for temporal lights, including fires and boats. Following Li et al. (2020), we use an empirical threshold of 0.3 $nWcm^{-2}sr^{-1}$ to remove dim light noises caused by these forms of temporal lights. The threshold is subtracted from the VIIRS image and negative pixel values are set to zero. This noise removal operation is conducted using Google Earth Engine. For our analysis, we use cloud free data, and assess if zero values in the average radiance imagery for our sample of cities

effectively encode no lights, as regions towards the poles during summer months have no data due to solar illumination. As a result, imagery for six time points is excluded from the analysis (SM Fig. 1).

The result is a series of monthly global composites for between December 2019 and June 2020 (Fig. 1). Each pixel within the image represents an area of 450 m^2. In analysing changes in NTL intensity, it is necessary to assume that these changes are the result of COVID-19 and associated restrictions; however, we acknowledge that other factors could have contributed (e.g. national holidays, blackouts and seasonal variations). As a result, as explained below, we further contextualise the imagery with additional indicator data sets: daily national estimates of stringency of government response (Hale et al., 2021); population density estimates (Stevens et al., 2015); confirmed COVID-19 cases (Ritchie et al., 2020); and daily sub-regional mobility estimates (Google, 2020).

2.2. Measuring city-scale changes in night-time lighting

To measure the overall extent of changes in energy consumption patterns in cities, we compute three summary indicators. All three indicators are based on the difference between the radiance for individual months and for December (our baseline). The first indicator is the mean number of pixels (Eq. (1)). It indicates the number of pixels defining individual cities that record a change on average across pixel differences for individual months (m_t) and the baseline month (m_0) (i.e. December 2019). Averages are computed conditionally for pixels indicating negative, neutral and positive change (C). The second indicator is the average percentage of pixels in each category: negative, neutral and positive (Eq. (2)). This indicator accounts for variations in city size to enable comparisons across cities. The third indicator is the median radiance (r) of night-time intensity across the difference from the baseline for each of the six months. This indicator provides an estimate of the total change in NTL intensity in individual cities, as well as the overall direction of this change (i.e. positive and negative). For this indicator we report only two categories (i.e. positive and negative), as the median for the neutral category is zero. In addition to these indicators, we analys the full distribution of the difference in NTL radiance between individual months and December 2019. Given small numbers, extreme NTL scores (i.e. above 30) are set to 30.

$$n = \frac{\sum_{t=1,m\in C}^{6} m_t\left(C\right) - m_0\left(C\right)}{6} \tag{1}$$

$$p = \frac{\sum_{t=1,m\in C}^{6} \frac{m_t(C) - m_0(C)}{m_t - m_0}}{6} \tag{2}$$

$$n = \frac{\sum_{t=1,m\in C}^{6} median\left[r_t\left(C\right) - r_0\left(C\right)\right]}{6} \tag{3}$$

To define city extents, we use the Functional Urban Area (FUA) boundaries developed during the Organisation for Economic Co-operation and Development and the Global Human Settlement layer project (Schiavina et al., 2019). Delimiting the extent of cities is challenging, and the FUA boundaries overcome this problem providing a consistent way to define extents based on population density measured at a fine spatial resolution (1 km^2 grids). First, adjacent grids of high density are clustered together. Then the level of commuting flows is measured to integrate non-continuous areas that display a distinctive urban centre of employment.

2.3. Analysing intra-urban changes in night-time lighting

To understand intra-urban changes, we conduct two sets of analyses. First, we examine the association between population density and NTL intensity using Generalised Additive Models (GAMs). We assess whether more densely populated areas in cities experience larger average declines in NTL intensity, arguably reflecting the location of employment centres. To this end, population density data are obtained from the WorldPop project (https://www.worldpop.org). These data comprise a raster layer covering the entire world and provide population density estimates at 1 km^2 grids. The data set is based on the United Nations' population count data using a top-down methodological approach (Stevens et al., 2015). In this approach, population counts at administrative units level are disaggregated to grid-cell based counts by using a series of detailed geospatial data sets, such as land cover, night-time imagery and proximity to amenities as covariates in a random forest estimation framework.

In a second analysis, we assessed the spatial distribution of NTL change between January and June 2020. We mapped the changes in NTL intensity for individual cities, and classify them based on the spatial structure of these changes during the month local lockdowns were enacted, or the following month if lockdowns were introduced towards the end of a month (SM Table 2 provides a list of start dates of local lockdowns for each city). We categorise cities into three classes: whole city, fragmented and spatially concentrated patterns of change. Whole city change encompasses cities displaying widespread dimmed or brightened patterns of NTL intensity. Fragmented change includes cities displaying scattered patterns of change. Spatially concentrated involves cities displaying geographically focused patterns of change. We observe three distinctive patterns: (1) changes along network infrastructures; (2) a core-periphery configuration; and, (3) systematic localised changes in key areas of cities.

2.4. Modelling mobility, stringency and COVID-19 infection

We also seek to understand the temporal patterns of urban energy use, non-pharmaceutical interventions and COVID-19 incidence. We use a hierarchical two-level modelling approach to capture time-city level interactions at level 1 and city-specific patterns at level 2. Monthly NTL data afford very limited temporal granularity, so we used Google Mobility Report data to capture these dynamics. The percentage change in stay-at home population is used as a proxy for shifts in urban energy use. We argue that this is a reasonable proxy as we expect that increases in stay-at-home population and simultaneous drops in time spent at work over time will likely be associated with changes in the patterns of urban energy use. Analysis of Google workplace and residential mobility data reveals that increases in stay-at-home population mirror declines in time spent at work (SM Fig. 4).

We estimate a series of hierarchical regression models using the percentage change of stay-at-home population as a function of a stringency indicator and COVID-19 incidence in a generalised linear mixed model (GLMM) framework. Intuitively, all estimated models include a stringency indicator and COVID-19 incidence measured at time t, and a stringency indicator at time $t-1$ recognising the delayed effects of lockdowns on influencing mobility patterns. For interpretation and identification purposes, independent variables are standardised, subtracting the mean and dividing by the standard deviation. We use natural splines to account for systematic temporal variations in the data, and incorporate natural splines as overall and city-specific parameters. We also include a temporal autoregressive term to account for temporal dependency. We evaluate the inclusion of temporal lags of higher order for the stringency indicator and COVID-19 incidence. Correlation coefficients and estimates for these variables are very small in size and statistical significance. We report a correlation matrix and two models in the SM Table 3 and Fig. 5 providing evidence for this.

More formally, we present evidence from three different model specifications in the manuscript (Fig. 5). These models are mathematically formulated in Eqs. (4)–(6): y_{it} captures change in stay-at-home population at city i in time t; β_{0i} is the random intercept that varies across cities; β_{1i} is the slope of the associated stringency indicator s_{it}; β_{2i} is the slope of the lagged stringency indicator at $t-1$; β_{3i} is the slope of new COVID-19 cases c_{it}; $\sum_{k=1}^{n+1}\beta_{ki}B_{kit}$ represents random natural spline

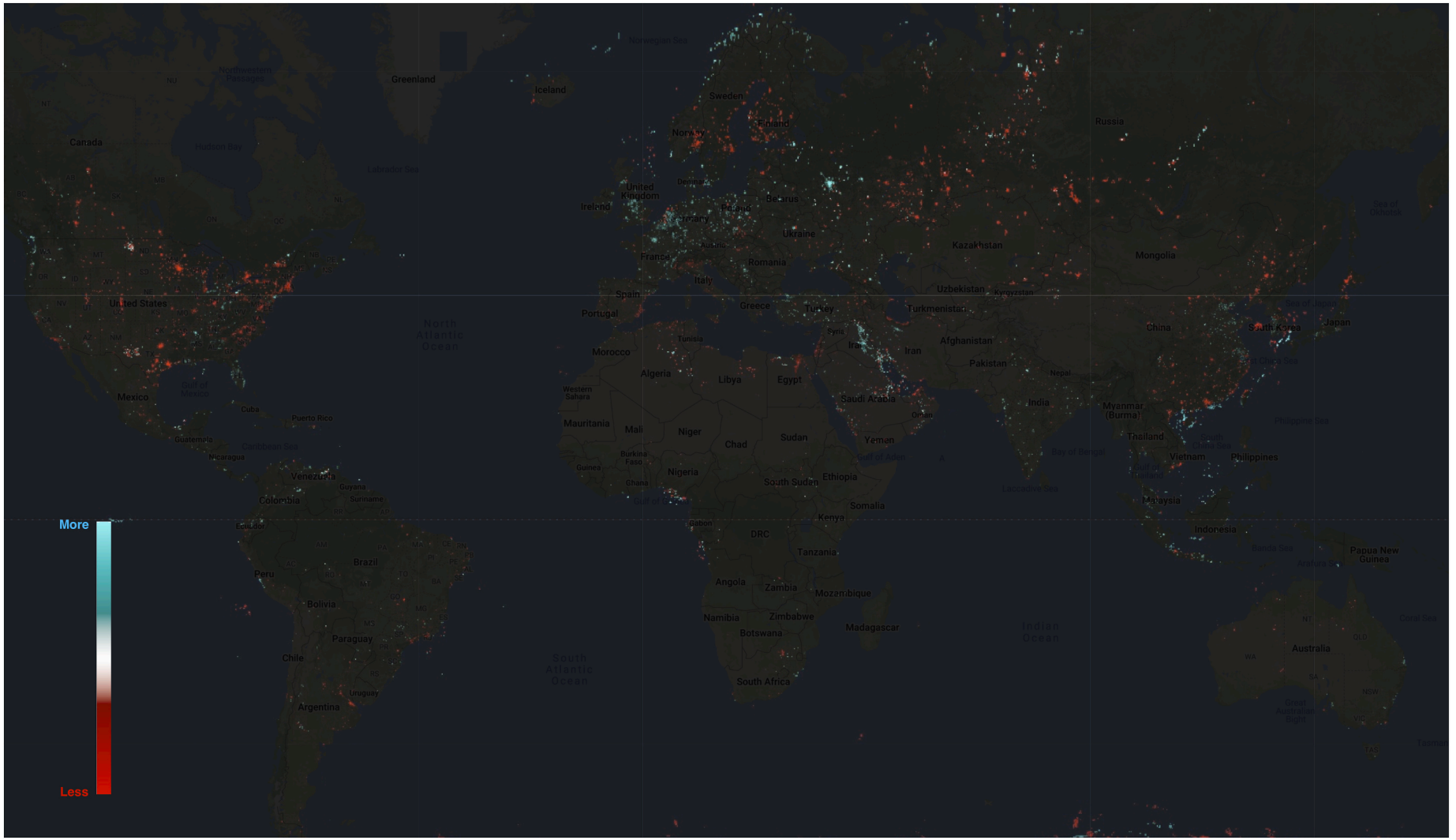

Fig. 1. Global map of NTL intensity. Difference in radiance between December 2019 and March 2020. Red encodes a reduction in NTL intensity (i.e. dimmed). Blue encodes an increase (i.e. brightened). NTL imagery is extracted from the Payne Institute for Public Policy (https://payneinstitute.mines.edu/eog/nighttime-lights/). (For interpretation of the references to colour in this figure legend, the reader is referred to the web version of this article.)

slopes at three knot points that vary across cities and capture systematic temporal patterns in stay-at-home population changes (see Hastie et al. (2009) for details on splines); ε_{it} is the city-time-level residual term that is assumed to be of first-order autoregressive (Ω_ε); that is, residuals are assumed to be correlated. Residuals at time $t-1$ are assumed to influence residuals at time t. Equations relating to β_{0i} and β_{ki} correspond to the random effects, or city-varying intercept and natural spline slopes, respectively. They capture variations in the associated parameters across cities and have unexplained heterogeneity denoted by u_{0i} and u_{ki}. These error terms follow an independent normal distribution $N(0,\sigma^2_{u0})$ and $N(0,\sigma^2_{u1})$.

$$\begin{aligned} y_{it} &= \beta_{0i} + \beta_{1i}s_{it} + \beta_{2i}s_{it-1} + \beta_{3i}c_{it} + \sum_{k=1}^{n+1}\beta_{ki}B_{kit} + \varepsilon_{it} \\ \beta_{0i} &= \beta_0 + u_{0i} \\ \beta_{ki} &= \beta_k + u_{ki} \\ \varepsilon_{it} &\sim N(0,\Omega_\varepsilon) \end{aligned} \tag{4}$$

The key difference across Eqs. (4)–(6) is in the parameter allowed to vary across cities. In Eq. (4), natural spline parameters are allowed to vary across cities capturing differences of systematic temporal fluctuations in stay-at-home population. We report the estimates for β_{1i}, β_{2i} and β_{3i} from this model as it provides the smallest Akaike Information Criterion (*AIC*) score. Though coefficients across all three models are fairly consistent in size. In Eq. (5), β_{1i} is allowed to vary across cities. This coefficient captures differences in the association between changes in stay-at-home population and the stringency indicator. In Eq. (6), β_{3i} is allowed to vary across cities. This coefficient captures differences in the association between changes in stay-at-home population and new COVID-19 cases. In addition, Eq. (6) also includes a lagged term (β_{4i}) for new COVID-19 cases to capture the lagging effect in the relationship between changes in stay-at-home population and new COVID-19 cases. All models included natural spline parameters in the fixed part of the model and a first-order autoregressive error term is assumed for the city-time level residuals.

$$\begin{aligned} y_{it} &= \beta_{0i} + \beta_{1i}s_{it} + \beta_{2i}s_{it-1} + \beta_{3i}c_{it} + \sum_{k=1}^{n+1}\beta_{ki}B_{kit} + \varepsilon_{it} \\ \beta_{0i} &= \beta_0 + u_{0i} \\ \beta_{1i} &= \beta_1 + u_{1i} \\ \varepsilon_{it} &\sim N(0,\Omega_\varepsilon) \end{aligned} \tag{5}$$

$$\begin{aligned} y_{it} &= \beta_{0i} + \beta_{1i}s_{it} + \beta_{2i}s_{it-1} + \beta_{3i}c_{it} + \beta_{4i}c_{it-1} + \sum_{k=1}^{n+1}\beta_{ki}B_{kit} + \varepsilon_{it} \\ \beta_{0i} &= \beta_0 + u_{0i} \\ \beta_{3i} &= \beta_3 + u_{3i} \\ \varepsilon_{it} &\sim N(0,\Omega_\varepsilon) \end{aligned} \tag{6}$$

During the modeling work, we draw on three additional contextual datasets: Google mobility data; Stringency Index and COVID-19 cases. Each dataset is now described in turn. *Google Mobility Data*: In response to COVID-19, Google released Community Mobility Reports to help inform public health responses to COVID-19 (https://www.google.com/covid19/mobility/). The data set measures the change in the number of visitors (or time spent) in relation to a baseline period. The baseline corresponds to the median value from the 5–week period January 3–February 6, 2020. The changes are categorised according to specific places or sectors: retail and recreation; groceries and pharmacies; parks; transit stations; workplaces; and residential. We focus our analysis on the residential category which indicates the change in stay-at-home population.

Stringency index: We use a stringency index to capture the level and variation of non-pharmaceutical interventions (https://covidtracker.bsg.ox.ac.uk). The stringency index is a composite indicator based on nine response indicators: school closures; workplace closures; cancellation of public events; restrictions on gatherings; public transport restrictions; public information campaigns; and stay at home measures (Hale et al., 2021). The index, available since 1st January 2020, computes a simple score by adding together the nine indicators which is rescaled to vary between 0 and 100. The stringency index is intended for comparative purposes, rather than as an indicator of how effective national policies have been at tackling the spread of COVID-19 (Hale et al., 2021).

COVID-19 cases: Data on the number of COVID-19 cases are obtained from Our World in Data (Ritchie et al., 2020). We also analyse the relationship between COVID-19 deaths and changes in stay-at-home population. We do not report these analyses in the main manuscript as we argue that COVID-19 cases are a more prominent measure of public knowledge in the early stages of the pandemic. We believe that individual responses during this period are more likely the result of the extent and rate of spread of COVID-19, rather than the actual number of deaths. We do however report analysis on COVID-19 in the SM Figs. 3 and 4.

3. Results and discussion

3.1. City-scale changes in energy consumption patterns during COVID-19

Comparison of imagery from December 2019 and each month between January 2020 and June 2020 yields three city-scale summary indicators of average NTL intensity (see Methods and Supplementary Materials (SM) Table 1), each a proxy for changes in urban energy consumption (Fig. 2). Firstly, the mean number of pixels indicator (left) indicates the proportion of pixels in each city for which the average change is either negative, neutral or positive. To account for variation in city size (with indicators based on number of pixels likely prioritising larger, less dense urban conurbations), a second indicator is provided based on the mean percentage of pixels (centre). Thirdly, an indicator of median percentage change illustrates the strength of change in NTL intensity (positive or negative). Based on the summary indicators, there is considerable variation in changes in energy consumption between selected cities.

Based on the mean percentage of pixels, in selected cities a high proportion of pixels experienced no change in NTL intensity during the six month period. In four cities this represented over half of pixels: Manila (53 %) Osaka (60 %), Melbourne (69 %) and Dhaka (74 %). Elsewhere, the mean percentage of pixels was overwhelmingly negative: Shanghai (56 %), Beijing (51 %); Johannesburg (54 %), Luanda (53 %), and Milan (54 %). For several cities, particularly in the Middle East, change was largely positive, including Tehran (50 %), Moscow (55 %) and Baghdad (64 %). The strength of change also varies as reflected by the median percentage change indicator. In Lima there was a large difference between the median negative (−25 %) and positive percentage change (+22.75 %) indicating considerable diversity in NTL intensity across space and time.

For other cities, the distribution of change in pixels is relatively similar for each time period (e.g. Melbourne; Osaka; Manila) (Fig. 3) suggesting that the spatial distribution of NTL intensity is quite stable over time. In Melbourne there was little change over time, likely reflective of stringent border closures that enabled a national zero-COVID strategy (Phillips, 2021). In other cities, where there was greater variation in the distribution of change (e.g. Karachi, Tehran, Kinshasa, Mumbai) detailed examination of the intra-urban distribution of NTL intensity is useful.

3.2. Shifting spatial patterns of intra-urban energy consumption during COVID-19

Examination of the relationship between population density and NTL intensity (Fig. 4) provides insight into the intra-urban distribution of energy consumption in response to COVID-19. Much attention has been paid to the risk of infection in dense urban centres (Hamidi et al., 2020; Xu et al., 2021), particularly during the early stages of the outbreak. This

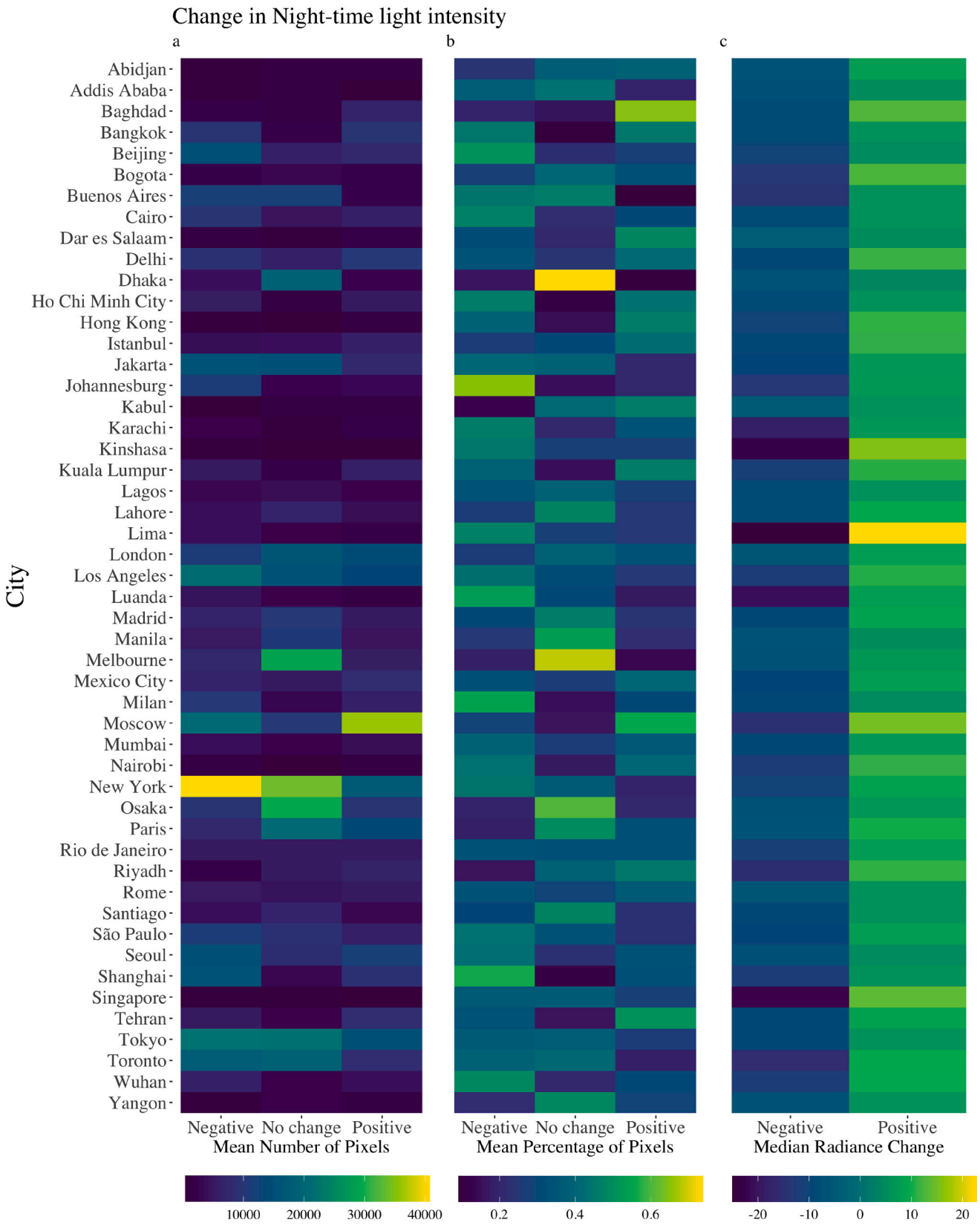

Fig. 2. Indicators of changes in NTL intensity. a Mean number of pixels: Average number of changing pixels. b Mean percentage of pixels. c Median radiance change: Median radiance of NTL intensity. These indicators refer to the difference between individual months (January 2020, February 2020, March 2020, April 2020, May 2020, and June 2020) and December 2019 across three categories: negative, neutral and positive. NTL imagery is extracted from the Payne Institute for Public Policy (https://payneinstitute.mines.edu/eog/nighttime-lights/).

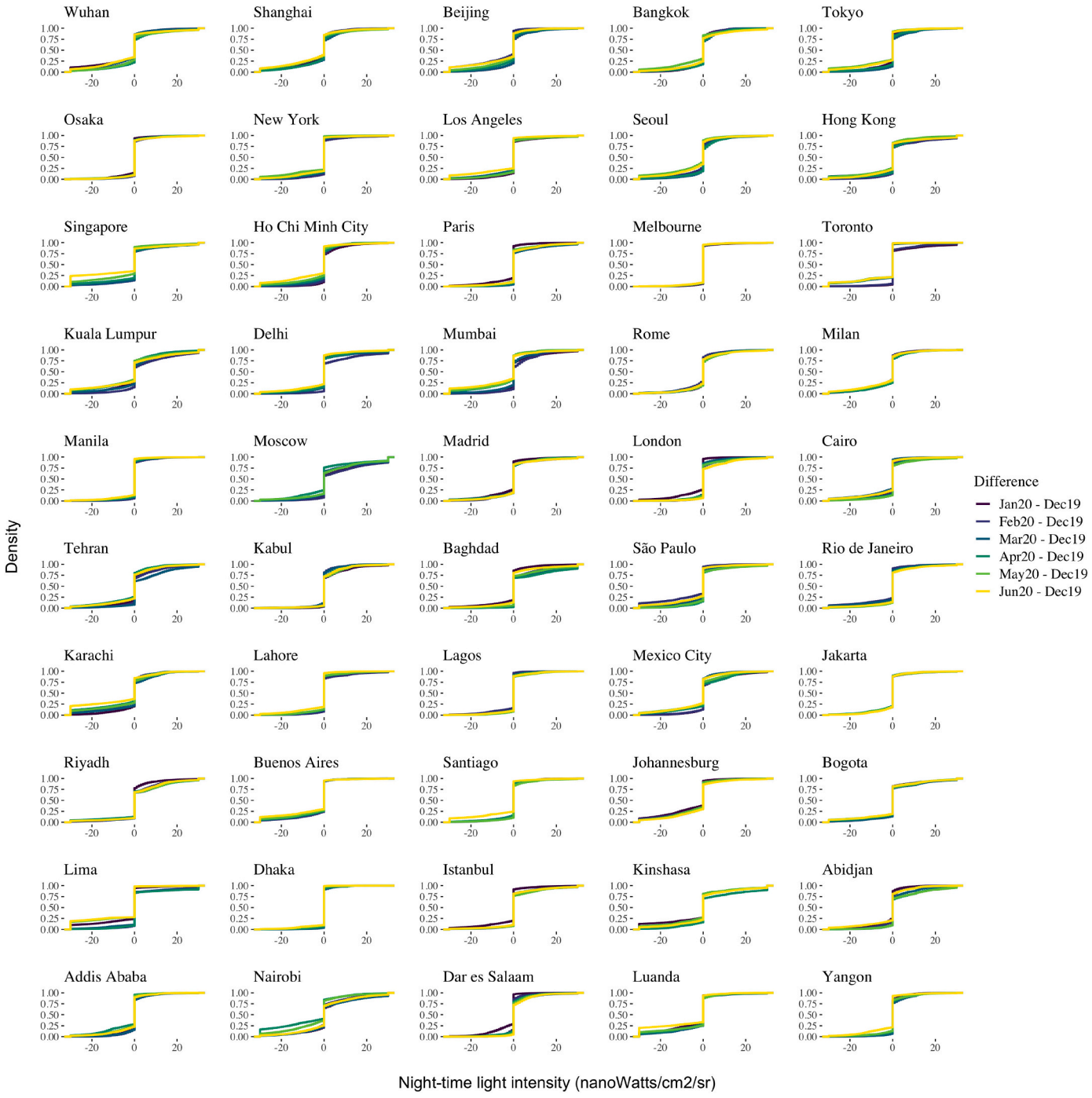

Fig. 3. Change in NTL intensity. Each line in the graph represents the difference in NTL intensity between each individual month (January 2020, February 2020, March 2020, April 2020, May 2020 and June 2020) and our baseline month (December 2019). The y-axis indicates the proportion of pixels at each value of the difference in night-time light intensity between relevant months. Comparing across density distributions provides an indication of the magnitude of change in night-time light intensity over time. NTL imagery is extracted from the Payne Institute for Public Policy (https://payneinstitute.mines.edu/eog/nighttime-lights/).

is evident in cities in which NTL intensity declined in densely populated areas (e.g. Johannesburg; Karachi; Kinshasa; Tokyo; Toronto). However, for the majority of cities we observe little association between the variables, with some cities experiencing a relative increase in light intensity in densely populated areas (e.g. Delhi, Melbourne; Rio de Janeiro; New York).

From closer inspection of mapped NTL intensity (for imagery for all 50 cities see SM Fig. 2), we identify three distinctive spatial configurations in energy use: (i) whole city; (ii) fragmented; and (iii) spatially concentrated (Fig. 5). This classification is not exhaustive, rather it illustrates the type, consistency and diversity of change in cities globally in response to COVID-19.

Firstly, selected cities experience a whole city change in NTL intensity. In Beijing, where a national lockdown was implemented in February, dimming of the majority of the pixels occurred (see also Addis Ababa; Beijing; Buenos Aires; Cairo; Luanda; Mexico City; Rio de Janeiro; São Paulo; Santiago; Shanghai; Toronto; Wuhan). Comparatively, in a small number of cities including Dar es Salaam, the majority of pixels brightened (see also Abidjan; Baghdad and Kabul). Secondly, selected cities experienced fragmented changes with pixels increasing

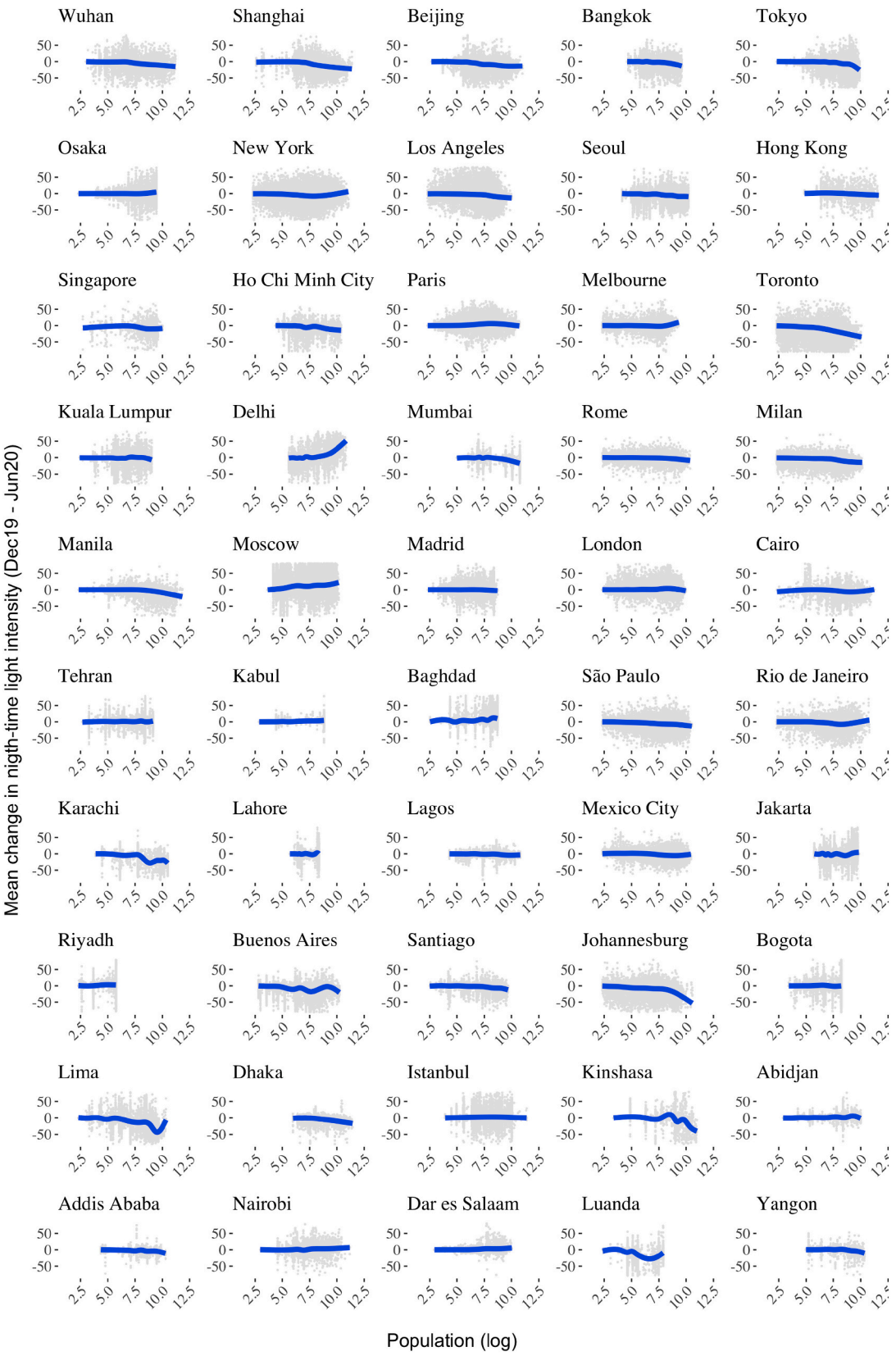

Fig. 4. Relationship between population density (log) and average change in NTL intensity. The average in NTL intensity corresponds to the difference across individual months (January–June 2020) and December 2019 (baseline). NTL imagery is extracted from the Payne Institute for Public Policy (https://payneinstitute.mines.edu/eog/nighttime-lights/). Population density data are obtained from the WordPop project (https://www.worldpop.org - see Stevens et al., 2015).

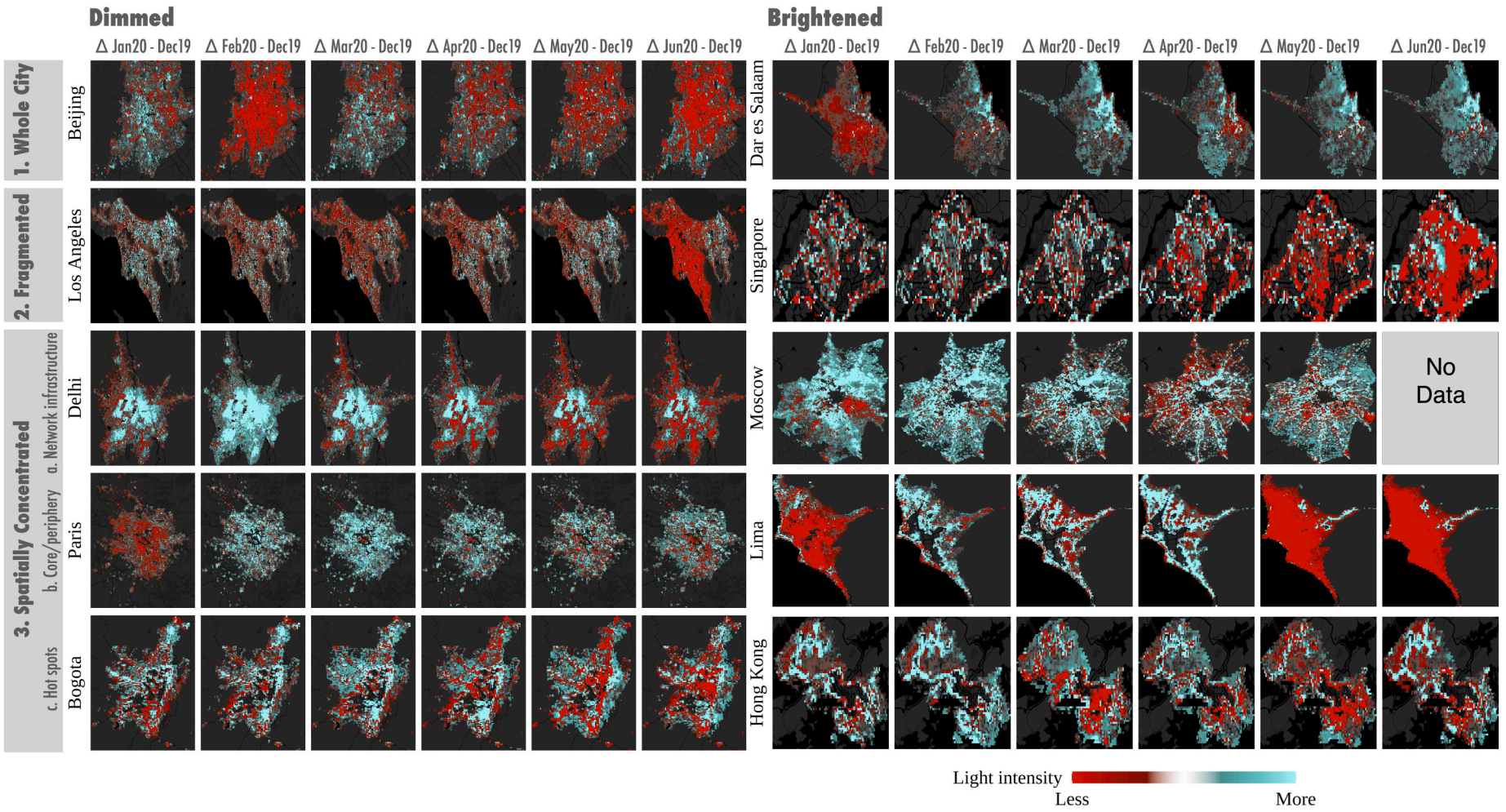

Fig. 5. Classification of global cities according to change in NTL intensity. Pixels shaded in red record a reduction NTL intensity (i.e. dimmed), whilst those shaded in blue record an increase (i.e. brightened). Areas that did not experience a change are not shaded. Interpretation of the imagery in the text is based on the month that national lockdown was first imposed in each city (SM Table 2). Where the date of lockdown was close to the end of the month, imagery for the following month is used. NTL imagery is extracted from the Payne Institute for Public Policy (https://payneinstitute.mines.edu/eog/nighttime-lights/). (For interpretation of the references to colour in this figure legend, the reader is referred to the web version of this article.)

and decreasing across the city with limited spatial patterning. This was the case in Los Angeles and Singapore when lockdown restrictions were introduced in March (see also Istanbul; Johannesburg; Kuala Lumpur; London; Melbourne; Milan; New York; Osaka; Rome; Singapore; Tokyo). Thirdly, spatially concentrated changes in NTL intensity also occur. Spatially concentrated changes are wide-ranging, reflecting diverse urban structures. Changes in some cities were shaped by networked infrastructures illustrative of connectivity (i.e. based on roads and economic corridors) that arguably play an integral role in the spread of COVID-19 (Hamidi et al., 2020). In Delhi, networked infrastructures dimmed in March in response to restrictions (see also Bangkok and Lahore), whilst in Moscow infrastructures brightened. Elsewhere, spatially concentrated forms of change replicated classic core-versus-periphery structures of cities (Dhaka; Karachi; Lagos; Madrid; Manila; Mumbai; Paris; Riyadh; Seoul; Tehran; Yangon). Yet in Lima, during March when lockdown was implemented, the core of the city brightened whilst the periphery dimmed. For some cities, hot spots of both dimming and brightening emerged (Bogota, Ho Chi Minh City; Hong Kong; Jakarta; Kinshasa Nairobi).

Where a whole city scale or spatially concentrated dimming of a city occurs, this is indicative of a variety of socio-spatial trends in response to COVID-19. Previous research on energy use and COVID-19 has evidenced substantial reductions in areas of concentrated economic activity. For example, there is evidence of heightened reductions in electricity consumption in areas with a high level of commercial activity (Ruan et al., 2020). As non-essential businesses close, schools and workplaces transition online and strict travel restrictions are implemented, evidence has also emerged of a transfer of energy consumption into the domestic sphere. For example, Liu et al. (2020) highlight increased activity in residential areas, decreased activities in commercial centres, and similar activity levels in transport and public facilities. In some cities a proportion of affluent or transient urban residents, no longer tied to places of employment, temporarily migrated away from dense urban areas where the perceived risks of contracting the virus are most acute (Connolly et al., 2020), thus contributing towards a suburbanisation of energy consumption. For example, in Wuhan where the virus first emerged, an estimated five million residents left the city prior to lockdown (Pinghui & Ma, 2020).

Further detailed analysis of cities with a spatially concentrated change offers insight into how NTL intensity is shaped by the degree and type of industrialisation in a city. Many highly industrialised areas - including energy intensive industrial zones and infrastructural corridors typically associated with high NTL intensity - experienced a concentrated reduction in energy consumption, as non-essential manufacturing halted during the pandemic. For example, in Wuhan, energy intensity reduced dramatically in the Optics Valley of China, the largest producer of fiber optic cable in the world, and the Wuhan subsidiary of the China Baowu Steel Corporation, one of the foremost global steel producers. Dimming of major energy infrastructures is also apparent, reflecting the role of global energy systems and markets in shaping urban energy intensity. For example, Riyadh Oil Refinery part of Saudi Aramco - a company with the world's second-largest proven crude oil reserves - dimmed as demand for oil hit a 25 year low in response to COVID-19 (Ambrose, 2020).

Yet as evidenced in the NTL imagery, some cities contradict more commonly documented trends of a reduction or suburbanisation of energy consumption. For example, in Dar es Salaam (a city that brightened overall) restrictions on socio-economic activities were relatively light-touch attributed to the political response to the pandemic (Makoni, 2021), coupled with concerns about impacts of lockdown on employment (Mfinanga et al., 2021). In selected cities, patterns also changed considerably over time. For example, in Lima one of the regions worst hit by COVID-19 (Munayco et al., 2020), a brightening of the core and dimming of the periphery from February until April gave way to a complete dimming in May and June.

3.3. Explaining changes in urban energy use through changes in mobility, stringency of government restrictions and COVID-19 incidence

Evidence of the diversity of configurations over both space and time suggests that multiple factors shape changes in urban energy consumption in response to COVID-19. We examine the association between temporal shifts in energy use patterns, and changes in COVID-19 incidence and non-pharmaceutical measures. We recognise the distinctive dynamics of this association across cities by employing a hierarchical two-level modelling approach, at level 1 capturing time-city interactions and level 2 capturing city-specific patterns (see Materials and methods section). Monthly NTL imagery affords limited temporal granularity, so we use Google Mobility Report data to capture these dynamics. Changes in mobility, specifically in the share of stay-at-home population, serve as a proxy for shifts in urban energy use (Mohammadi & Taylor, 2017). To measure non-pharmaceutical interventions, we use a stringency index which is a composite indicator that measures the extent and variation of non-pharmaceutical interventions globally, ranging from 0 (no measures) to 100 (the strictest scenario) (Hale et al., 2021).

We recognise two important features in the association between these factors. First, the relationship between changes in mobility (energy use), COVID-19 incidence and non-pharmaceutical measures represents multiple causal mechanisms, arising from "top-down" government interventions and "bottom-up" individual responses. For instance, strict non-pharmaceutical measures may result in business and school closures, reducing mobility, increasing the share of stay-at-home population, and ultimately domestic energy consumption. Conversely, rising COVID-19 case transmission, particularly early in the pandemic, may have led to increasing public concern fuelled by anxiety and fear with a rising number of stay-at-home population and domestic energy usage as a result of reduced workplace activity.

Second, these relationships exhibit different temporal dynamics across cities (Fig. 6a and b). Certain cities (Melbourne, Kuala Lumpur, Delhi, Manila, Lagos) display large increases in stay-at-home population associated with strict non-pharmaceutical interventions despite relatively small rises in COVID-19 cases. Cities like Singapore, Paris, Madrid, Santiago and Lima show equally large increases in stay-at-home population and strict interventions; yet report consistently high numbers of COVID-19 cases. Others, including Bangkok and Seoul, display moderate increases in stay-at-home population despite strict non-pharmaceutical interventions.

Fig. 6c–e reports our modelling of changes in the share of stay-at-home population as a function of stringency intervention and new COVID-19 cases (see Methods and SM Table 3 for full model estimates). Main fixed effects are displayed in Fig. 6c, and random, varying city slopes for stringency and new COVID-19 cases in Fig. 6d–e, respectively. Compared to COVID-19 cases, a larger and positive estimate for local stringency measures ($\beta = 4.69$;95 % $CI = 3.85 - 5.52$) (Fig. 6c) suggests that the enactment of "top-down" stringent lockdown played a major role in incentivising working from home and hence domestic energy consumption across most cities in our sample. Coupled with a positive but smaller estimate for local stringency at time t-1 ($\beta = 2.73$;95 % $CI = 2.02 - 3.45$), these findings also suggest that the largest impact of stringency measures on reducing travel-to-work activity was immediate but it takes some time for this to be fully realised.

Fig. 6d–e reveals the extent of variation in the association between changes in the share of stay-at-home population, and stringency measures and new COVID-19 cases across our sample of cities. Cross-tabulating estimates for these associations, we identify four groupings of cities (Fig. 6f):

- Group one includes cities with greater than average stringency and COVID-19 cases estimates, (e.g. Kuala Lumpur, Manila and Mumbai). Underpinning these results are relatively high shares of stay-at-home population (40 %) and arguably domestic energy use, coupled with

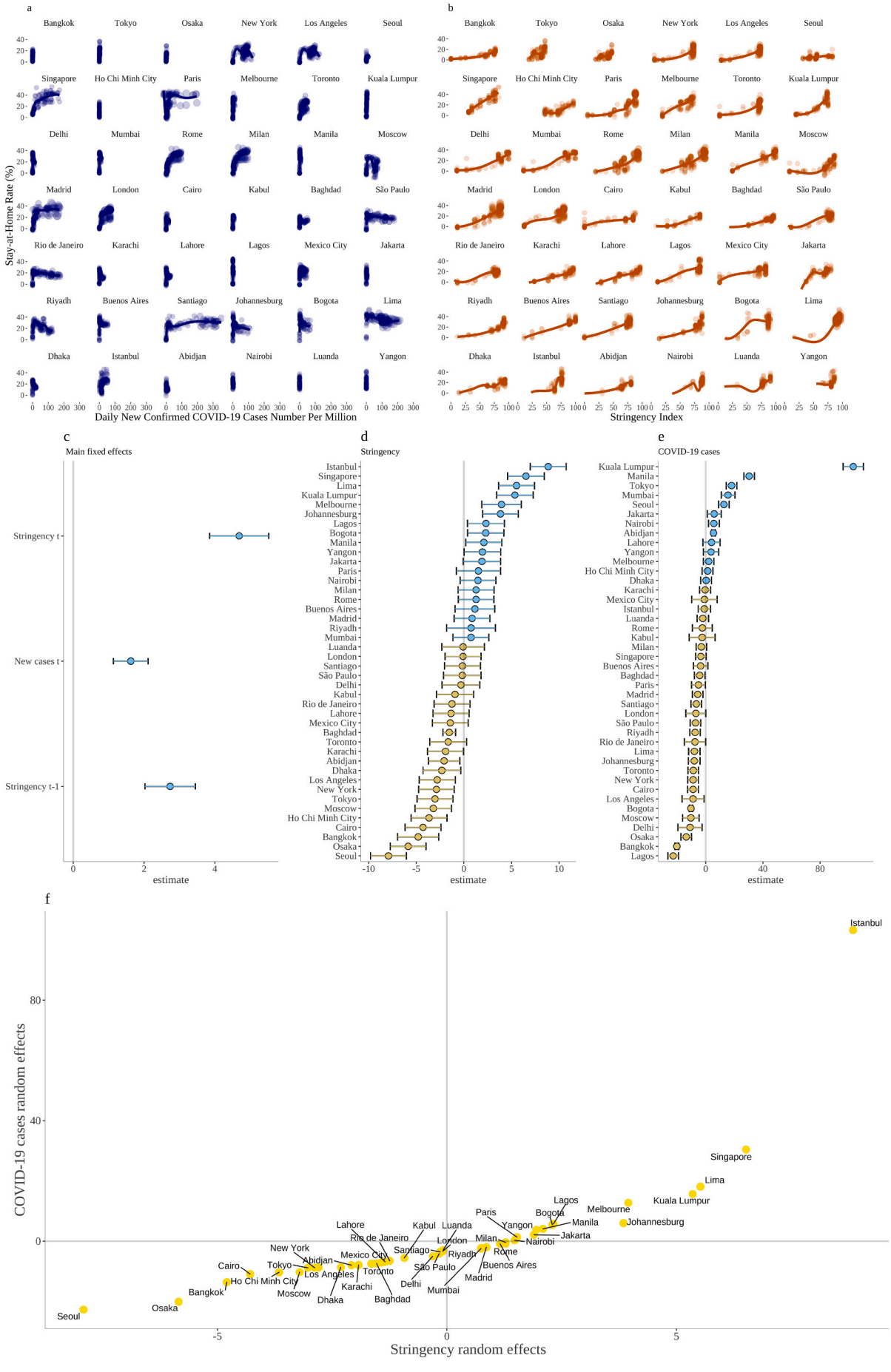

(caption on next page)

Fig. 6. Association between stay-at-home population, stringency and COVID-19 cases. a Relationship between stay-at-home population and new COVID-19 cases per million. b Relationship between stay-at-home population and stringency index. c Regression coefficients: main fixed effects were obtained from Eq. (4). d Regression coefficients: random effects for stringency across cities were obtained from Eq. (5). e Regression coefficients: random effects for COVID-19 cases across cities were obtained from Eq. (6). f Classification based on stringency and COVID-19 cases random effects estimated via Eqs. (5) and (6).

high levels of stringency (100) and continuously small numbers of COVID-19 cases (<15 per million) (Fig. 6a–b).

- Group two displays larger than average stringency but lower COVID-19 cases estimates (e.g. Lagos, Bogota, Lima and Johannesburg). This reflects initially large and subsequently moderate increases in stay-at-home population (ranging from 40 %–20 %) and domestic energy use, and moderate rises in COVID-19 cases despite strict lockdown interventions early in the pandemic (i.e. March) (Fig. 6a–b and SM Table 3).
- Group three includes cities with smaller than average stringency and COVID-19 case estimates (e.g. Bangkok, Osaka, Cairo, Moscow and New York). These cities display moderate rises in the share of stay-at-home population (<25 %) and domestic energy use despite stringent measures, with varying outcomes of COVID-19 cases: persistently low in Bangkok, Osaka and Cairo, and relatively high in Moscow and New York.
- Group four comprises a small set of cities displaying small stringency but greater than average COVID-19 cases estimates (e.g. Seoul and Tokyo). These patterns reflect a trend of moderate stay-at-home population shares (<20 %), low COVID-19 cases and stringency measures. In South Korea, transmission was controlled by employing less stringent social distancing measures than in Europe and the United States (Watanabe & Yabu, 2021). Similarly, Japan did not impose stringent lockdown measures, but enacted a state of emergency strategy to encourage people to stay at home (Dighe et al., 2020).

These overarching trends suggest that "top-down" emergency restrictions and legislation introduced by national governments have played a substantial role in reconfiguring social and economic structures, and therefore energy consumption patterns, in the majority of cities selected. However, where government response has been relatively light touch, "bottom-up" changes in energy–related practices owing to the response of individuals or employers to the crisis assume greater importance in shaping energy consumption (Schot et al., 2016). In the absence of emergency legislation, people are still required to engage in essential everyday activities that encourage energy consumption e.g. commuting. However, our results show that energy consumption and mobility declined moderately over time, as non-essential energy-related activities were foregone in response to the increased incidence of COVID-19.

4. Conclusions

Energy production, demand consumption is highly locally contingent and spatially uneven (Baka & Vaishnava, 2020; Broto & Baker, 2018). Analysis of socio-spatial datasets can provide unique insights into the geographical distribution of energy consumption at a range of scales (Bouzarovski & Thomson, 2018; Robinson et al., 2019). In our analysis of energy consumption during COVID-19 using NTL imagery, whilst global, and typically national, demand for energy fell overall in response to COVID-19 and accompanying restrictions (especially in contexts where per-capita energy use is typically high) (IEA, 2021) new spatial distributions have emerged between and within cities.

Our analysis provides a global assessment of the city-scale changes in energy consumption patterns during COVID-19, evidencing considerable variations in changes across the largest 50 urban agglomerations in the world. For some cities, changes in energy consumption as indicated by NTL intensity are overwhelming negative in response to COVID-19, yet elsewhere the reverse pattern is observed. We also provide evidence of three distinctive signatures of changes in the spatial patterns of intra-urban energy consumption within cities, reflecting widespread and more localised geographical changes across the urban landscape. This evidence expands existing predominant narratives suggesting the "suburbanisation" of energy demand in several urban contexts during the early phases of COVID-19 as the dominant spatial pattern of energy usage as lockdowns were enacted, business and services were closed, and home working became the predominant form of employment (Abdeen et al., 2021; Krarti & Aldubyan, 2021; Qarnain et al., 2020). We provide evidence that suburbanisation is just one of several distinctive ways in which energy consumption has been reconfigured within large cities across the globe.

We also presented statistical evidence suggesting that, whilst variability exists, government stringency responses to mitigate the spread of COVID-19 were a key factor in shaping changes and reductions in urban energy consumption observed in most cities in our sample during the early stages of the pandemic. Individual behavioural responses to minimise exposure to COVID-19 also appeared to have resulted in higher local shares of stay-at-home population and hence declines in urban energy consumption in cities, but to a lesser extent. Taken together, these findings suggest that structural policy responses are key to generate large-scale changes in energy use, and support the need for ambitious national and global policies that substantially reconfigure social and economic systems, rather than individual behaviour change - if the necessary scale of change for a low-carbon society is to be achieved. Our study thus contributes to the ongoing debate about whether COVID-19 is likely to act as a catalyst for a permanent reduction in urban energy consumption owing to digitalisation of work and other activities (Kanda & Kivimaa, 2020), and indeed as inspiration for transitions to a low carbon society (Henry et al., 2020).

Our analysis evidences changes in the spatial patterns of urban energy use during night-time as encoded in NTL satellite imagery based on lighting from urban features and mobility. Overall, domestic energy consumption increased during the pandemic; the most significant change is in the shape of the load profiles during the day time as household schedules and day-time mobility patterns change. Further research is thus needed to capture these shifts in demand for energy during the day and understand the energy-related household practices or industrial energy usage underpinning these changes as estimates of energy consumption become available. Our analysis focuses on large global urban conurbations. Understanding changes in energy patterns in smaller cities or rural and peri-urban areas is also important as these areas recorded a large influx of population moving away from high density areas, suggesting a transfer of energy demand from urban agglomerations to smaller areas (González-Leonardo, López-Gay, Newsham, Recaño, & Rowe, 2022; González-Leonardo, López-Gay, Recaño Valverde, & Rowe, 2022; Rowe et al., 2022).

Additionally, our analysis captures changes in the spatial distribution of urban energy during COVID-19. Whilst these changes may largely reflect, as we believe, the effects of lockdowns, they may also reflect seasonal variations in the distribution of population across cities as some parts of the world transitioned from winter into spring. More importantly, identifying the causes of changes in energy consumption observed in large cities over the early stages of the pandemic and extending the period of analysis could be key to better understand the extent to which the changes brought about by COVID-19 are temporary or will endure as hybrid working becomes ingrained in societies. Evidence of changes in energy consumption post-lockdown suggests that recovery to pre-lockdown levels is socially and spatially uneven, with relatively affluent areas experiencing a rapid recovery compared to

poorer regions (Aruga et al., 2020; Zheng et al., 2020). Detailed spatial analyses of NTL imagery beyond June 2020 could provide insight into the longer-term impacts of COVID-19, including inequalities embedded in the recovery of energy consumption levels post-lockdown.

CRediT authorship contribution statement

F.R. and C.R. devised the project, the main conceptual ideas, proof outline and wrote the first draft. F.R. and N.P. collected the data performed, design the data visualisations, developed code and conducted the night-time light imagery analysis. F.R. performed the modelling analysis. F.R., C.R. and N.P. discussed the results, revised the manuscript and approved the final version.

Data availability

The data used for our analysis is publicly available online: monthly VIIRS NTL satellite imagery composites (version 1) from the Earth Observations Group (EOG) Payne Institute for Public Policy, https://eogdata.mines.edu/download_dnb_composites.html; daily COVID-19 pandemic data from Our World in Data, https://github.com/owid/covid-19-data/tree/master/public/data; social distancing and lockdown data from the Oxford COVID-19 Government Response Tracker (OxCGRT), https://github.com/OxCGRT/covid-policy-tracker; Google mobility data, https://www.google.com/covid19/mobility/; and, global population data from the WorldPop project, https://www.worldpop.org/project/categories?id=18. The results supporting the findings of this study are provided in the main text and Supplementary information. The source data underlying all the figures in the main manuscript and Supplementary information are provided as a Source Data file. Source data to replicate the results reported in the paper are provided in an Open Science Framework (OSF) repository, DOI: https://doi.org/10.17605/OSF.IO/P74QR, except for the monthly VIIRS NTL imagery composites which exceed the data storage capacity in GitHub. VIIRS NTL composites can be obtained from the first link provided in this paragraph.

Code availability

The code to reproduce all the analysis and figures reported in this study are openly available in an Open Science Framework (OSF) repository, DOI: [10.17605/OSF.IO/P74QR] (https://doi.org/10.17605/OSF.IO/P74QR). The analysis was performed in RStudio 1.3.959 running on R version 4.0.2 (2020-06-22) using the following list of packages sorted in alphabetical order: “countrycode 1.2.0”, “corrplot 0.84”, “glmmTMB 1.0.2.1”, “ggpubr 0.4.0”, “grid 4.0.2”, “gridExtra 2.3”, “lubridate 1.7.9”, “osmdata 0.1.3”, “raster 3.3-13”, “rvest 0.3.6”, “sf 0.9-5”, “tmaptools 3.1”, “tidyverse 1.3.0”, “viridis 0.5.1”. Refer to the README in the repository for instructions.

Declaration of competing interest

The authors declare that there is no conflict of interest.

Acknowledgements

This study was supported by the UKRI Future Leaders Fellowship grant (MR/V021672/1).

Appendix A. Supplementary Material

Supplementary material to this article can be found online at https://doi.org/10.1016/j.cities.2022.103808.

References

Abdeen, A., Kharvari, F., O’Brien, W., & Gunay, B. (2021). The impact of the COVID-19 on households’ hourly electricity consumption in Canada. *Energy and Buildings, 250*, Article 111280. https://doi.org/10.1016/j.enbuild.2021.111280

Acuto, M., Larcom, S., Keil, R., Ghojeh, M., Lindsay, T., Camponeschi, C., & Parnell, S. (2020). Seeing COVID-19 through an urban lens. *Nature Sustainability, 3*, 977–978. https://doi.org/10.1038/s41893-020-00620-3

Ambrose, J. (). *Oil prices slump as markets face lowest demand in 25 years*. Available at https://www.theguardian.com/business/2020/apr/15/oil-prices-slump-as-market-faces-lowest-demand-in-25-years-covid-19. The Guardian (online; accessed 19-February-2021).

Arribas-Bel, D., Green, M., Rowe, F., & Singleton, A. (2021). Open data products-a framework for creating valuable analysis ready data. *Journal of Geographical Systems, 23*(4), 497–514. https://doi.org/10.1007/s10109-021-00363-5

Arribas-Bel, D., Rowe, F., Chen, M., & Comber, S. (2022). “An image library” The potential of imagery in regional science. In S. Rey, & R. Franklin (Eds.), *Handbook of spatial analysis in the social sciences* (pp. 1–25). Edward Elgar (in press).

Aruga, K., Islam, M. M., & Jannat, A. (2020). Effects of COVID-19 on Indian energy consumption. *Sustainability, 12*(14), 5616. https://doi.org/10.3390/su12145616

Bahmanyar, A., Estebsari, A., & Ernst, D. (2020). The impact of different COVID-19 containment measures on electricity consumption in Europe. *Energy Research & Social Science, 68*. https://doi.org/10.1016/j.erss.2020.101683

Baka, J., & Vaishnava, S. (2020). The evolving borderland of energy geographies. *Geography Compass, 14*(7), Article e12493. https://doi.org/10.1111/gec3.12493

Batty, M. (2020). The coronavirus crisis: What will the post-pandemic city look like? *Environment and Planning B: Urban Analytics and City Science, 47*(4), 547–552. https://doi.org/10.1177/2399808320926912

Beyer, R. C., Franco-Bedoya, S., & Galdo, V. (2021). Examining the economic impact of COVID-19 in India through daily electricity consumption and nighttime light intensity. *World Development, 140*. https://doi.org/10.1016/j.worlddev.2020.105287

Bouzarovski, S., & Thomson, H. (2018). Energy vulnerability in the grain of the city: Toward neighborhood typologies of material deprivation. *Annals of the American Association of Geographers, 108*(3), 695–717. https://doi.org/10.1080/24694452.2017.1373624

Brosemer, K., Schelly, C., Gagnon, V., Arola, K. L., Pearce, J. M., Bessette, D., & Olabisi, L. S. (2020). The energy crises revealed by COVID: Intersections of indigeneity, inequity, and health. *Energy Research & Social Science, 68*, Article 101661. https://doi.org/10.1016/j.erss.2020.101661

Broto, V. C., & Baker, L. (2018). Spatial adventures in energy studies: An introduction to the special issue. *Energy Research & Social Science, 36*, 1–10. https://doi.org/10.1016/j.erss.2017.11.002

Broto, V. C., & Kirshner, J. (2020). Energy access is needed to maintain health during pandemics. *Nature Energy, 5*, 2058–7546. https://doi.org/10.1038/s41560-020-0625-6

Brunsdon, C., & Comber, A. (2021). Opening practice: Supporting reproducibility and critical spatial data science. *Journal of Geographical Systems, 23*(4), 477–496. https://doi.org/10.1007/s10109-020-00334-2

Bustamante-Calabria, M., Sánchez de Miguel, A., Martín-Ruiz, S., Ortiz, J.-L., Vílchez, J. M., Pelegrina, A., … Gaston, K. J. (2021). Effects of the COVID-19 lockdown on urban light emissions: Ground and satellite comparison. *Remote Sensing, 13*, 2072–4292. https://doi.org/10.3390/rs13020258

Cao, C., Xiaoxiong, X., Wolfe, R., DeLuccia, F., Liu, Q. M., Blonski, S., … Hillger, D. (2017). NOAA technical report NESDIS 142 visible infrared imaging radiometer suite (VIIRS) sensor data record (SDR) user’s guide version 1.3. In *NOAA technical report NESDIS 142* (pp. 1–40).

Carvalho, M., de Mello Delgado, D. B., de Lima, K. M., de Camargo Cancela, M., dos Siqueira, C. A., & de Souza, D. L. B. (2021). Effects of the COVID-19 pandemic on the Brazilian electricity consumption patterns. *International Journal of Energy Research, 45*, 3358–3364. https://doi.org/10.1002/er.5877

Chen, C.-F., de Rubens, G. Z., Xu, X., & Li, J. (2020). Coronavirus comes home? Energy use, home energy management, and the social-psychological factors of COVID-19. *Energy Research & Social Science, 68*, 22146296. https://doi.org/10.1016/j.erss.2020.101688

Connolly, C., Ali, S. H., & Keil, R. (2020). On the relationships between COVID-19 and extended urbanization. *Dialogues in Human Geography, 10*, 2043–8206. https://doi.org/10.1177/2043820620934209

Dighe, A., Cattarino, L., Cuomo-Dannenburg, G., Skarp, J., Imai, N., Bhatia, S., … Riley, S. (2020). Response to COVID-19 in South Korea and implications for lifting stringent interventions. *BMC Medicine, 18*, 1741–7015. https://doi.org/10.1186/s12916-020-01791-8

Elvidge, C. D., Baugh, K. E., Zhizhin, M., & Hsu, F.-C. (2013). Why VIIRS data are superior to DMSP for mapping nighttime lights. *Proceedings of the Asia-Pacific Advanced Network, 35*(0), 62. https://doi.org/10.7125/APAN.35.7

Gebreslassie, M. G. (2020). COVID-19 and energy access: An opportunity or a challenge for the African continent? *Energy Research & Social Science, 68*, 22146296. https://doi.org/10.1016/j.erss.2020.101677

Geels, F. W., Sovacool, B. K., Schwanen, T., & Sorrell, S. (2017). The socio-technical dynamics of low-carbon transitions. *Joule, 1*, 25424351. https://doi.org/10.1016/j.joule.2017.09.018

Gillingham, K. T., Knittel, C. R., Li, J., Ovaere, M., & Reguant, M. (2020). The short-run and long-run effects of Covid-19 on energy and the environment. *Joule, 4*, 25424351. https://doi.org/10.1016/j.joule.2020.06.010

González-Leonardo, M., López-Gay, A., Newsham, N., Recaño, J., & Rowe, F. (2022). Understanding patterns of internal migration during the COVID-19 pandemic in Spain. *Population, Space and Place*. https://doi.org/10.1002/psp.2578

González-Leonardo, M., López-Gay, A., Recaño Valverde, J., & Rowe, F. (2022). Changes of residence in times of COVID-19: A small respite from rural depopulation. *Perspectives Demogràfiques, 26*, 1–4.

Google. (2020). Google COVID-19 community mobility reports. Available at https://www.google.com/covid19/mobility/ (01/07/2021).

Green, M., Pollock, F. D., & Rowe, F. (2021). New forms of data and new forms of opportunities to monitor and tackle a pandemic. In G. J. Andrews, V. A. Crooks, J. R. Pearce, & J. P. Messina (Eds.), *COVID-19 and similar futures* (pp. 423–429). Springer. https://doi.org/10.1007/978-3-030-70179-6_56.

Hale, T., Angrist, N., Goldszmidt, R., Kira, B., Petherick, A., Phillips, T., Webster, S., Cameron-Blake, E., Hallas, L., Majumdar, S., & Tatlow, H. (2021). A global panel database of pandemic policies (Oxford COVID-19 Government Response Tracker). *Nature Human Behaviour, 5*, 2397–3374. https://doi.org/10.1038/s41562-021-01079-8

Hamidi, S., Sabouri, S., & Ewing, R. (2020). Does density aggravate the COVID-19 pandemic? *Journal of the American Planning Association, 86*, 0194–4363. https://doi.org/10.1080/01944363.2020.1777891

Hastie, T., Tibshirani, R., & Friedman, J. (2009). *The elements of statistical learning*. New York: Springer. https://doi.org/10.1007/978-0-387-84858-7

Henry, M. S., Bazilian, M. D., & Markuson, C. (2020). Just transitions: Histories and futures in a post-COVID world. *Energy Research & Social Science, 68*, 22146296. https://doi.org/10.1016/j.erss.2020.101668

International Energy Agency. (2020). The COVID-19 crisis is causing the biggest fall in global energy investment in history. In *Technical report*. International Energy Agency (IEA).

International Energy Agency. (2021). Global energy review 2021. In *Technical report*. International Energy Agency (IEA).

International Monetary Fund. (2021). World economic outlook update, April 2021. In *Technical report*. International Monetary Fund (IMF).

Kanda, W., & Kivimaa, P. (2020). What opportunities could the COVID-19 outbreak offer for sustainability transitions research on electricity and mobility? *Energy Research & Social Science, 68*, 22146296. https://doi.org/10.1016/j.erss.2020.101666

Krarti, M., & Aldubyan, M. (2021). Review analysis of COVID-19 impact on electricity demand for residential buildings. *Renewable and Sustainable Energy Reviews, 143*, Article 110888. https://doi.org/10.1016/j.rser.2021.110888

Kuzemko, C., Bradshaw, M., Bridge, G., Goldthau, A., Jewell, J., Overland, I., … Westphal, K. (2020). COVID-19 and the politics of sustainable energy transitions. *Energy Research & Social Science, 68*, 22146296. https://doi.org/10.1016/j.erss.2020.101685

Levin, N., Kyba, C. C., Zhang, Q., de Miguel, A. S., Román, M. O., Li, X., , … Miller, S. D., et al. (2020). Remote sensing of night lights: A review and an outlook for the future. *Remote Sensing of Environment, 237*, Article 111443. https://doi.org/10.1038/s41597-020-0510-y

Li, X., Zhou, Y., Zhao, M., & Zhao, X. (2020). A harmonized global nighttime light dataset 1992–2018. *Scientific Data, 7*(1), 1–9. https://doi.org/10.1038/s41597-020-0510-y

Liu, Q., Sha, D., Liu, W., Houser, P., Zhang, L., Hou, R., Lan, H., Flynn, C., Lu, M., Hu, T., & Yang, C. (2020). Spatiotemporal patterns of COVID-19 impact on human activities and environment in mainland China using nighttime light and air quality data. *Remote Sensing, 12*, 2072–4292. https://doi.org/10.3390/rs12101576

Makoni, M. (2021). Tanzania refuses COVID-19 vaccines. *The Lancet, 397*, 01406736. https://doi.org/10.1016/S0140-6736(21)00362-7

Memmott, T., Carley, S., Graff, M., & Konisky, D. M. (2021). Sociodemographic disparities in energy insecurity among low-income households before and during the COVID-19 pandemic. *Nature Energy, 6*, 2058–7546. https://doi.org/10.1038/s41560-020-00763-9

Mfinanga, S. G., Mnyambwa, N. P., Minja, D. T., Ntinginya, N. E., Ngadaya, E., Makani, J., & Makubi, A. N. (2021). Tanzania's position on the COVID-19 pandemic. *The Lancet, 397*, 01406736. https://doi.org/10.1016/S0140-6736(21)00678-4

Miller, S., Straka, W., Mills, S., Elvidge, C., Lee, T., Solbrig, J., … Weiss, S. (2013). Illuminating the capabilities of the Suomi National Polar-Orbiting Partnership (NPP) visible infrared imaging radiometer suite (VIIRS) day/night band. *Remote Sensing, 5*. https://doi.org/10.3390/rs5126717

Min, B., Gaba, K. M., Sarr, O. F., & Agalassou, A. (2013). Detection of rural electrification in Africa using DMSP-OLS night lights imagery. *International Journal of Remote Sensing, 34*(22), 8118–8141. https://doi.org/10.1080/01431161.2013.833358

Mohammadi, N., & Taylor, J. E. (2017). Urban energy flux: Spatiotemporal fluctuations of building energy consumption and human mobility-driven prediction. *Applied Energy, 195*. https://doi.org/10.1016/j.apenergy.2017.03.044

Munayco, C. V., Tariq, A., Rothenberg, R., Soto-Cabezas, G. G., Reyes, M. F., Valle, A., , … Chowell, G., et al. (2020). Early transmission dynamics of COVID-19 in a southern hemisphere setting: Lima-Peru: February 29th–March 30th, 2020. *Infectious Disease Modelling, 5*, 338–345. https://doi.org/10.1016/j.idm.2020.05.001

Norouzi, N., de Rubens, G. Z., Choupanpiesheh, S., & Enevoldsen, P. (2020). When pandemics impact economies and climate change: Exploring the impacts of COVID-19 on oil and electricity demand in China. *Energy Research & Social Science, 68*, 22146296. https://doi.org/10.1016/j.erss.2020.101654

Phillips, N. (2021). The coronavirus is here to stay—Here's what that means. *Nature, 590*.

Pinghui, J., & Ma, Z. (2020). *5 million left wuhan before lockdown, 1,000 new coronavirus cases expected in city*.

Qarnain, S. S., Sattanathan, M., Sankaranarayanan, B., & Ali, S. M. (2020). Analyzing energy consumption factors during coronavirus (COVID-19) pandemic outbreak: A case study of residential society. In *Energy sources, part a: Recovery, utilization, and environmental effects* (pp. 1–20). https://doi.org/10.1080/15567036.2020.1859651

Ritchie, H., Mathieu, E., Rodés-Guirao, L., Appel, C., Giattino, C., Ortiz-Ospina, E., Hasell, J., Macdonald, B., Beltekian, D., & Roser, M. (2020). *Coronavirus pandemic (COVID-19)*. Our World in Data. https://ourworldindata.org/coronavirus.

Robinson, C., Lindley, S., & Bouzarovski, S. (2019). The spatially varying components of vulnerability to energy poverty. *Annals of the American Association of Geographers, 109*(4), 1188–1207. https://doi.org/10.1080/24694452.2018.1562872

Román, M. O., Stokes, E. C., Shrestha, R., Wang, Z., Schultz, L., Carlo, E. A. S., , … Kalb, V., et al. (2019). Satellite-based assessment of electricity restoration efforts in Puerto Rico after Hurricane Maria. *PLoS One, 14*(6), Article e0218883. https://doi.org/10.1371/journal.pone.0218883

Rowe, F., Calafiore, A., Arribas-Bel, D., Samardzhiev, K., & Fleischman, M. (2022). *Understanding the patterns of human mobility in Britain during the COVID-19 pandemic using Facebook data*. preprint (pp. 1–17).

Ruan, G., Wu, D., Zheng, X., Zhong, H., Kang, C., Dahleh, M. A., … Xie, L. (2020). A cross-domain approach to analyzing the short-run impact of COVID-19 on the US electricity sector. *Joule, 4*, Article 25424351. https://doi.org/10.1016/j.joule.2020.08.017

Schiavina, M., Moreno-Monroy, A., Maffenini, L., & Veneri, P. (2019). GHSL-OECD functional urban areas. In *Technical report*. Publications Office of the European Union.

Schot, J., Kanger, L., & Verbong, G. (2016). The roles of users in shaping transitions to new energy systems. *Nature Energy, 1*, 2058–7546. https://doi.org/10.1038/nenergy.2016.54

Stevens, F. R., Gaughan, A. E., Linard, C., & Tatem, A. J. (2015). Disaggregating census data for population mapping using random forests with remotely-sensed and ancillary data. *PLoS One, 10*, 1932–6203. https://doi.org/10.1371/journal.pone.0107042

United Nations. (2018). Work urbanization prospects 2018: Highlights. In *Technical report*. United Nations.

Wang, Z., Román, M., Sun, Q., Molthan, A., Schultz, L., & Kalb, V. (2018). Monitoring disaster-related power outages using NASA black marble nighttime light product. In *ISPRS Int. Arch. Photogramm. Remote Sens. Spat. Inf. Sci* (pp. 1853–1856).

Watanabe, T., & Yabu, T. (2021). Japan's voluntary lockdown. *PLoS One, 16*, 1932–6203. https://doi.org/10.1371/journal.pone.0252468

Werth, A., Gravino, P., & Prevedello, G. (2021). Impact analysis of COVID-19 responses on energy grid dynamics in Europe. *Applied Energy, 281*, Article 116045. https://doi.org/10.1016/j.apenergy.2020.116045

Xu, G., Xiu, T., Li, X., Liang, X., & Jiao, L. (2021). Lockdown induced night-time light dynamics during the COVID-19 epidemic in global megacities. *International Journal of Applied Earth Observation and Geoinformation, 102*, 03032434. https://doi.org/10.1016/j.jag.2021.102421

Zheng, B., Geng, G., Ciais, P., Davis, S. J., Martin, R. V., Meng, J., … Zhang, Q. (2020). Satellite-based estimates of decline and rebound in China's CO2 emissions during COVID-19 pandemic. *Science Advances, 6*, 2375–2548. https://doi.org/10.1126/sciadv.abd4998